RSC Advances

PAPER

View Article Online
View Journal | View Issue

Cite this: *RSC Adv.*, 2025, **15**, 1125

Unidirectional moisture-conducting green fabrics prepared by a one-step electrospray technique

Shumin Bi, †[a] Yueru Yang,†[a] Guangling Pei,[a] Tianci Yang,[b] Shui Hu*[b] and Qingxiu Jia *[a]

Received 22nd November 2024
Accepted 5th January 2025

DOI: 10.1039/d4ra08289c

rsc.li/rsc-advances

Unidirectional moisture-conducting fabrics were prepared by electrospraying polyvinylidene fluoride (PVDF) and polyvinyl chloride (PVC) onto three green fabric substrates, namely cotton, hemp, and modal. Experiments were conducted to examine the effects of coating thickness, coating material, and substrate material on the moisture conductivity of the fabrics. The electrospraying technique was effective in forming uniform and strongly adhered PVDF and PVC coatings on the fabric substrates, and the coating thickness and material type had a significant effect on the fabric's moisture conductivity. The PVDF and PVC coatings significantly improved the unidirectional moisture conductivity of the fabric substrates, and although the unidirectional moisture conductivity effects differed among the substrates, all fabrics exhibited high directional water transport capacities (*R* values greater than 300%), high air permeabilities, and high water vapor transmission rates. Cotton and hemp substrates coated with hydrophobic layers showed more efficient unidirectional moisture transfer than modal fabrics. This study demonstrated that appropriate coating design and substrate selection can significantly improve the moisture conductivity of fabrics, providing a valuable reference for the development of high-performance functional textiles.

1. Introduction

Functional textiles have received increasing attention in recent years. Among them, unidirectional moisture-conducting fabrics have become a research hotspot owing to their wide application in sportswear, outdoor equipment, and medical textiles.[1] Maintaining the moisture and thermal balance of the human body is one of the critical factors influencing textile comfort, but traditional textiles have a single performance that makes it difficult to combine moisture conduction and heat dissipation simultaneously.[2,3] Furthermore, sweat plays an important role in regulating human moisture and heat.[4] If the sweat produced by the human body cannot be discharged from the body through the fabric, the humidity of the microclimate between the skin and the fabric increases, and the moisture on the skin increases, causing discomfort, as well as causing the air between the fibers to be squeezed out, resulting in a drop in temperature. Unidirectional moisture-conducting fabrics can effectively transfer the sweat from the skin to the outer layer while blocking moisture from transferring in the opposite direction, thereby keeping the human body dry and comfortable.

The process of directional water transfer mainly depends on the asymmetric wettability of the material.[5,6] There are two main methods to develop unidirectional moisture-conducting fabrics. One is to rationally design the fabric structure by combining hydrophobic fibers with hydrophilic fibers and constructing a wetting gradient or differential capillary effect by adjusting the thickness.[7,8] The other is to construct a wettability gradient by modifying the textile surface through finishing processes, such as single-sided coating,[4,9,10] plasma treatment,[11,12] laser modification,[13] and electrospinning.[5,14,15] Most commercially available moisture-conducting fabrics rely on the composite or post-finishing technology of polymer materials, which have poor environmental protection and involve complex processes. Therefore, it is necessary to develop an efficient and simple method for manufacturing moisture-conducting fabrics.

Electrostatic spraying (*i.e.*, electrospraying) is an advanced process widely used in the field of coating. It enables the on-demand deposition of functional materials[16] and has the advantages of high efficiency, uniformity, and material savings. Electrospraying provides a uniform coating on the surface of textiles and enhances the bonding force between the coating and the substrate,[17] thereby imbuing textiles with additional functionality. Moreover, the charge of the droplets can be controlled by changing the voltage and flow rate, thereby adjusting the coating thickness, which is significant in the construction of functional fabrics, particularly unidirectional moisture-conducting fabrics.[18]

[a]*School of Materials Design and Engineering, Beijing Institute of Fashion Technology, Beijing, China. E-mail: clyjqx@bift.edu.cn*

[b]*College of Materials Science and Engineering, Beijing University of Chemical Technology, Beijing, China. E-mail: hushui@mail.buct.edu.cn*

† Contributed equally to this work.

There are several reports on the preparation of unidirectional moisture-conducting textiles by electrospraying. For example, Chen *et al.*[19] prepared high-performance directional water-conducting textiles using a three-step strategy that involved electrospinning oriented polyacrylonitrile on polylactic acid nonwoven surface, dipping the fabrics in hydrophilic reagents, and electrospraying polyvinylidene fluoride (PVDF) solution on one side of the fabric. The prepared hydrophilic oriented polyacrylonitrile (HOPAN)/hydrophilic polylactic acid @polyvinylidene fluoride (HPLA@PVDF) fiber membrane exhibited high directional water transport performance (accumulative one-way transport capacity (R) = 1117%, overall moisture management capacity (OMMC) = 0.91). Cheng *et al.*[20] combined electrospinning and electrospraying to prepare Janus textiles, which consisted of hydrolyzed polyacrylonitrile (HPAN)/hexagonal boron nitride nanosheets (BNNS) fibrous membrane with small pores and hydrophilicity, conductive Ag nanowire (NW)layer and polyurethane (TPU) nanofibrous membrane with large pores and hydrophobicity. The textiles showed a dual gradient in terms of the pore size and wettability in the thickness direction, achieving directional perspiration performance. These recent studies have mostly used electrostatic spraying technology in combination with other methods. Although previous studies have used one-step electrospraying techniques to prepare unidirectional moisture-conducting fabrics, they focused on the quantitative analysis of the liquid transport performance, such as changing the thickness of the hydrophobic coating and the pore size of the hydrophilic fabric substrate.[21,22] Notably, there is a lack of reports that comprehensively investigate the effects of coating type, fabric substrate type, and coating thickness on the performance of unidirectional moisture-conducting fabrics.

In this study, three different types of green hydrophilic fabrics, namely cotton, hemp, and modal, were used as substrate materials. A simple and efficient one-step electrospraying technique was employed to form a hydrophobic coating on one side of these fabrics, creating a significant wetting gradient difference between the two sides. The feasibility of achieving unidirectional moisture-conducting performance in the fabrics *via* electrospraying was systematically verified, providing new insights for the development of multifunctional green unidirectional moisture-conducting textiles.

2. Materials and methods

2.1 Materials

PVDF powder (M_w = 300 000) was kindly provided by Arkema Inc.; PVC powder (M_w = 80 000) was purchased from Ningbo Formosa Plastics Industry Co., Ltd.; cotton cloth (weight of 124.1 g m^{-2}) was purchased from Yujin Textile; hemp cloth (weight of 133.4 g m^{-2}) was purchased from Youngor Textile Co., Ltd.; modal cloth (weight of 248.6 g m^{-2}) was custom-made; *N*,*N*-dimethylacetamide (DMAc; purity of 99.55%) was purchased from Shanghai Eon Chemical Technology Co., Ltd.; and calcium chloride (analytical grade) was purchased from Shanghai MacLean Biochemical Technology Co., Ltd.

2.2 Material preparation

First, 1.4 g of PVDF powder was weighed and dissolved in 10 ml of DMAc. After continuous stirring for 8 h at room temperature, it was allowed to stand for defoaming, resulting in a PVDF spinning solution. Similarly, the PVC spinning solution was prepared by dissolving 0.9 g of PVC powder in 10 ml of DMAc and leaving it to defoam after continuous stirring for 8 h at room temperature.

The fabric to be treated was soaked in 500 ml of deionized water until it was completely wetted and then suspended until no liquid droplets fell. Subsequently, the fabric was fixed on the electrospinning receiving roller. A certain amount of spinning solution was injected into a 10 ml syringe, and the distance between the needle and the receiving roller was set to 15 cm for PVC spinning solution and 12 cm for PVDF spinning solution, respectively. The solution was electrosprayed onto the fabric at a propulsion speed of 1 ml h^{-1} and a voltage of 12 kV, and the electrospraying time was set to 1, 2, and 3 h. Thus, the composite fabrics with asymmetric wettability were obtained. The fabrics were named PVC-C-*x*, PVC-H-*x*, PVC-M-*x*, PVDF-C-*x*, PVDF-H-*x*, and PVDF-M-*x*, where *x* represents the electrospraying time, and C, H, and M denote cotton, hemp, and modal, respectively.

2.3 Characterization

The morphologies of the composite fabric surfaces were observed by scanning electron microscopy (SEM; JSM-7500F, Japan). The chemical and elemental compositions of the composite fabrics were analyzed by Fourier transform infrared (FTIR) spectroscopy (Nicolet5700FT-IR, ThermoNicolet Corporation, USA) and energy-dispersive X-ray spectroscopy (EDS; XFlash 610M, Bruker, Germany). The water contact angle (WCA) was measured using an optical contact angle meter (OCA 20, Data-Physics GmbH, Germany). The thickness of the sample was measured using a thickness gauge (CHY-U, Jinan Sanquan Zhongshi Experimental Instrument Co., Ltd.). The air permeability was evaluated using an air permeability tester (FX3300-IV, TEXTEST, Switzerland). The unidirectional moisture conduction was quantitatively analyzed using a moisture management tester (M290, SDL Atlas, China), according to AATCC 195-2009. The water vapor transmission rate (WVT; g m^{-2} d^{-1}) was evaluated using a custom experimental setup. The sample was cut into a suitable size and fixed over the mouth of a beaker filled with deionized water, with the hydrophobic layer of the composite fabric facing down and the hydrophilic layer facing up. The beaker was placed in an oven at 30 °C for 1 h, and then the sample was removed and weighed. The final result was determined using the following formula:

$$\mathrm{WVT} = \frac{m_1 - m_2}{St}, \quad (1)$$

where $m_1 - m_2$ is the mass of water evaporated, S is the effective area of water vapor passing through the sample, and t is the test duration.

3. Results and discussion

3.1. Design of the one-way moisture-conducting fabric

Fig. 1 illustrates the preparation process of the unidirectional moisture-conducting composite fabrics. Three common fabrics, namely cotton, hemp, and modal, are first soaked in deionized water. This wetting process can improve the conductivity of the fabric surface, helping the polymer to adhere more strongly and evenly to the fabric surface. Then, hydrophobic PVDF and PVC spinning solutions are electrosprayed on one side of the pre-treated fabric to achieve a gradient from hydrophobic to hydrophilic in the thickness direction, thereby increasing the driving force for directional water transport.

3.2. Microstructure, surface chemical composition and wetting behavior

Fig. 2(a) shows the microstructure on the electrosprayed side of the resulting composite fabric. The surface of the control fabric (*i.e.*, the fabric without electrospraying) is relatively smooth, but after single-sided spraying treatment, a rough surface is observed, with a large number of tightly packed micro and nanoparticle bundles. This indicates the presence of PVDF and PVC on the fabric surface. As the electrospraying time increases, the number of particle bundles significantly increases, and the difference in surface roughness on both sides of the fabric also significantly increases, which enhances the hydrophobic performance to a certain extent. Therefore, by adjusting the electrostatic spraying time, the hydrophobic properties of one side of the fabric can be effectively controlled.

To analyze the chemical characteristics of the original fabric and composite fabric surfaces, FTIR analysis was performed (Fig. 2(b)). In the infrared spectra of all three fabrics, characteristic peaks were observed in the 3000–3500 cm^{-1} region, which were attributed to the –OH stretching vibration in cellulose. However, the shape and intensity of the peaks significantly changed after electrospraying treatment. After electrospraying PVC on the surface of cotton and modal fabrics, –OH may form various hydrogen bonds with PVC molecules and exert van der Waals forces, causing the characteristic peak to broaden. After electrospraying PVDF, the characteristic –OH peak weakened, which may simply occur because the fibers are covered. For hemp fabrics, both treatments lead to the broadening of the characteristic –OH peak and its shift in the lower wave number direction. At the same time, the peak intensity of each composite fabric after treatment was significantly enhanced near 1640 cm^{-1}. The broad and weak absorption peak seen here in untreated fabrics is generally attributed to the effects of water molecules and intramolecular hydrogen bonds in cellulose. When PVDF or PVC is coated on the fabric surface, the formation of intermolecular hydrogen bonds enhances the absorption peak. In addition, the C=O bonds present in PVC may shift because of changes in the chemical environment and overlap with the absorption peak at 1640 cm^{-1}, further enhancing the peak. For PVDF composite fabrics, characteristic peaks can be observed at 1401 and 1159 cm^{-1}, corresponding to the $-CH_2$ bending vibration and $-CF_2$ tensile vibration, respectively. The absorption peaks at 876 and 838 cm^{-1} are caused by the crystalline phase in PVDF, which is consistent with the literature.[23] These results indicate that the polymer is successfully attached to the fabric surface.

The elemental composition of the fabric surface was analyzed by EDS, and the results are shown in Fig. 2(c) and (d). According to the molecular structure of cellulose, it mainly contains C and O elements. After PVDF modification, F appeared on the fabric surface, which is unique to PVDF. Similarly, Cl appeared on the surface of the fabric after PVC modification. Furthermore, the results show that the elements are evenly distributed on the composite fabric surfaces.

3.3. Effects of the hydrophobic layers on the behavior of unidirectional moisture-conducting fabrics

The previous results examined the feasibility of preparing fabrics with gradient wettability by electrospraying. Next, we examined the influence of PVDF and PVC on the unidirectional moisture conduction performance of the composite fabrics. Water droplets with a volume of 2 μl were dropped on the

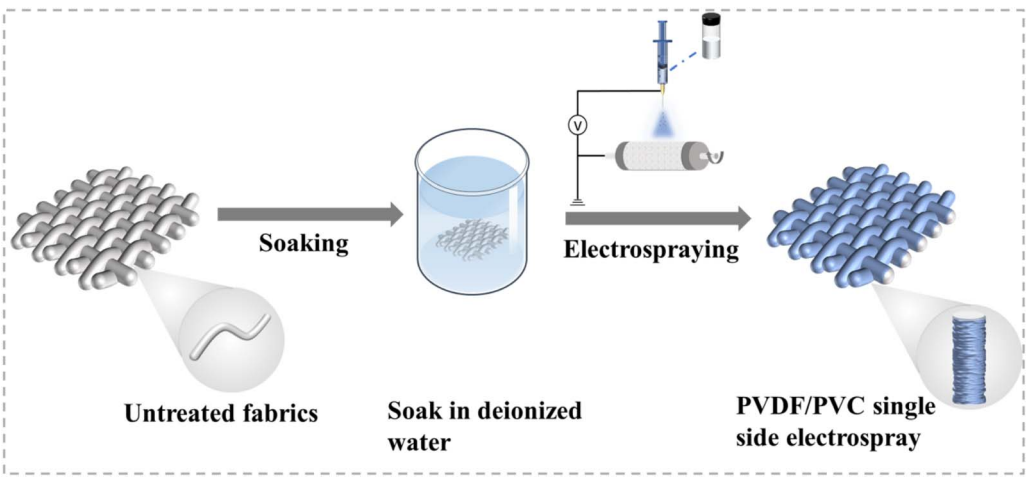

Fig. 1 Illustration of the process used for preparing and analyzing unidirectional moisture-conducting composite fabrics.

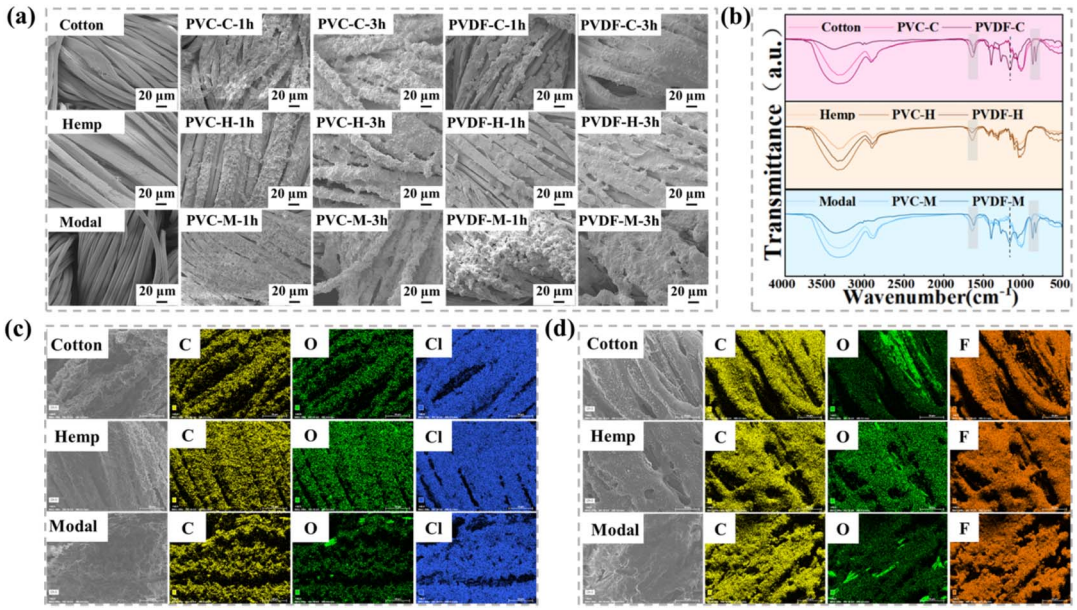

Fig. 2 (a) SEM images of the fabrics prepared with different electrospraying times. (b) FTIR spectra of the fabrics after 3 h of electrospraying. EDS spectra of the fabrics coated with (c) PVC and (d) PVDF.

sprayed side of the fabric, and a contact angle tester was used to determine the time required for the water droplets to transfer from the hydrophobic side to the hydrophilic side.

As shown in Fig. 3(a)–(f), the wettability of the fabric is affected by the thickness of the hydrophobic film. Nonetheless, the water droplets can be completely absorbed on the surface of all samples. Among them, the modal-based composite fabric provided faster absorption than the other two substrate materials. The water droplet disappearance times on PVC-M-1, PVC-M-2, and PVC-M-3 were 0.3, 0.3, and 6 s, and the water droplet disappearance times on PVDF-M-1, PVDF-M-2, and PVDF-M-3 were 0.7, 0.6, and 0.4 s, respectively. This is because the moisture absorption performance of the modal fabric is high, and the water droplets falling on the fabric surface are immediately

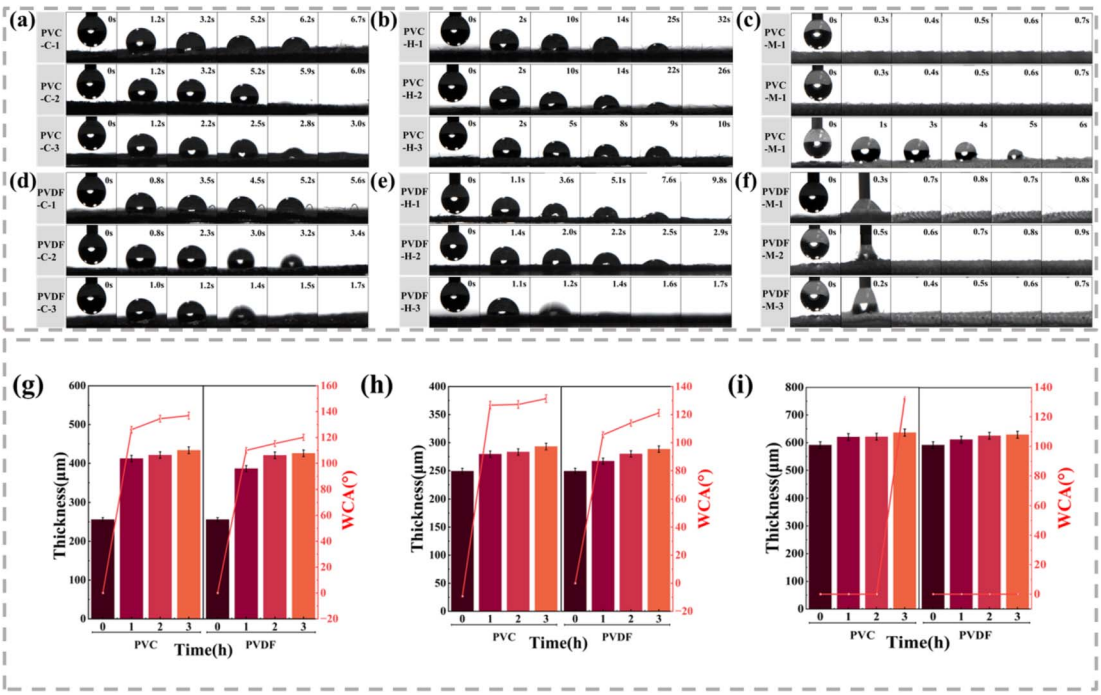

Fig. 3 (a–f) Changes in the water droplet shape and wettability on each composite fabric over time. (g–i) Fabric thicknesses and WCA values of the three composite fabrics after different electrostatic spraying times.

absorbed and diffused. Notably, it is not possible to use this test to determine the unidirectional conduction efficiency of these fabrics. However, when the water droplets fall on PVC-M-3, water droplet penetration can be observed.

Except for the modal-based composites, the water droplets falling on the hydrophobic side surface of the other composite fabrics remain spherical for some time and then vertically penetrate the fabric. As the electrospray time increases from 1 to 3 h, the disappearance time of the water droplets gradually shortens. Moreover, the thickness of the original cotton, hemp, and modal fabrics are 255.9, 249.2, and 522.0 μm, respectively (Fig. 3(g)–(i)). The thicknesses of the cotton and hemp composite fabrics increase with the extension of the electrospraying time, and the WCA on the spraying side also increases. Although the thickness of the modal composite fabric increases with the increase of the spraying time, the WCA remains at 0° owing to the high absorption rate. Additionally, compared with cotton and hemp fabrics, modal fabrics have more microporous structures inside. These tiny gaps can absorb and accommodate more water molecules, contributing to its hygroscopicity. The synergistic effect of absorption and penetration prevents water droplets from remaining on the fabric surface for even a short time. The introduction of both polymers effectively improves the WCA of the substrate material, and when the coating content increases, the hydrophobicity increases. The longer the spraying time, the more that the pores of the fabric become covered, which may effectively prevent the penetration of water molecules and enhance the hydrophobic performance. According to the Young–Laplace equation, the reduction in pore size leads to an increase in the Laplace force, thereby repelling water droplets, which means that the wettability gradient across the fabric is enhanced. In addition, from the morphology of the fabric, electrospraying results in a rough surface layer, thus forming a roughness difference in the thickness direction of the fabric. This roughness difference and the surface energy gradient both promote the transfer of water droplets along a specific direction.[24] Ultimately, the unidirectional moisture conduction behavior is maximized using a longer electrospraying time.

3.4. Asymmetric wetting behavior of unidirectional moisture-conducting fabrics

Asymmetric wettability is an important feature of unidirectional moisture-conducting fabrics; therefore, we evaluated the water transport process and WCA changes on both sides of the fabric, and the results are shown in Fig. 4. Considering the high water absorption rate of the modal fabric, no distinct change in the WCA can be observed, and thus it is not shown in the figure. For the cotton and hemp fabrics, the water droplet initially maintains a spherical shape on the hydrophobic side and then gradually penetrates the interior of the fabric. Furthermore, the three-phase line diagram indicates only vertical movement. Combined with the corresponding dynamic WCA change curve, the WCA drops sharply from more than 90° to 0° within 10 s, except for the PVDF-M sample where the WCA was always 0°. On the hydrophilic side, the water droplet quickly diffuses and disappears after contacting the fabric surface. The three-phase line moves to both sides, and the initial WCA is less than 90°, indicating hydrophilicity. The results show that water transfer from the hydrophobic side to the hydrophilic side is feasible, while the transport in the opposite direction may be hindered.

To observe the water transfer process, 10 μl of water was dropped on both sides of the fabric, and the change in the diffusion diameter of the water droplets over time was recorded, as shown in Fig. 5. When the water droplets fall on the hydrophobic side, the diameter becomes 0 mm within a certain period. However, the water droplets initially remain spherical, and at this time, the diffusion diameter is the diameter of the contact surface between the water droplets and the fabric surface. As the water droplets penetrate to the other side, they no longer contact the hydrophobic side, and the wetting diameter at this time is 0. Meanwhile, the diameter of the droplets on the hydrophilic side gradually increases from 0 mm to a fixed value. When the water droplets fall on the hydrophilic side, they diffuse rapidly; the diffusion diameter gradually increases and finally reaches the maximum value. However, owing to the hydrophobic force on the hydrophobic side, the water droplets cannot penetrate, and the diffusion diameter remains 0 mm on the hydrophobic side. These results confirm

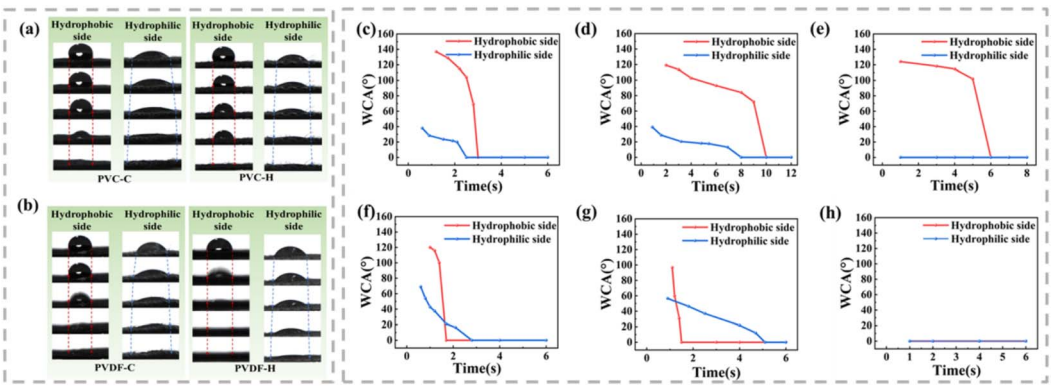

Fig. 4 (a and b) Changes in the shape of water droplets on composite fabrics with different hydrophobic layers prepared using an electrospraying time of 3 h. (c–e) For PVC, the changes in WCA over time are shown for cotton, hemp, and modal, from left to right. (f–h) For PVDF, the changes in WCA over time are shown for cotton, hemp, and modal, from left to right.

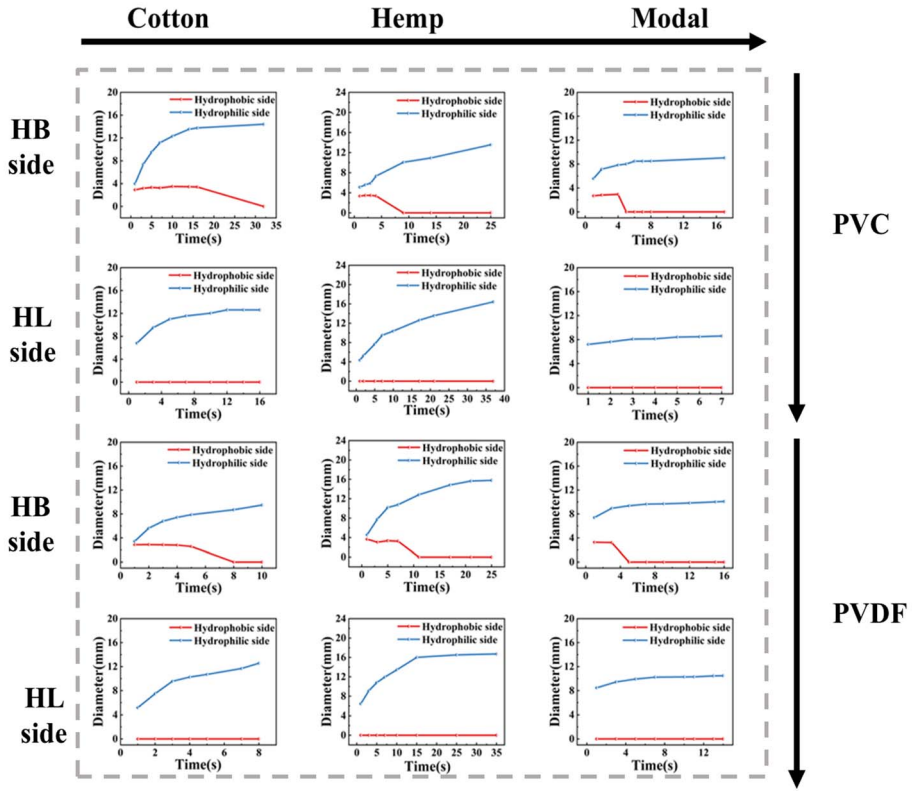

Fig. 5 Relationship between the water diffusion diameter and the time when water is dropped on the hydrophobic and hydrophilic sides of each fabric (HL represents the hydrophilic side and HB represents the hydrophobic side).

that when the water droplets contact the hydrophobic surface, they penetrate the fabric and remain on the hydrophilic surface. Therefore, in practical applications, the skin can be kept dry when the hydrophobic side is facing the skin.

Additionally, the directional moisture transport ability of the composite fabric was evaluated using a moisture management tester (MMT), in which water droplet landed on the hydrophobic side. The cumulative unidirectional transport index (R) is a key indicator for determining the directional water transport behavior of the material and can be calculated using the following formula, where T represents the test time, and U_t and U_b represent the moisture content at the top and bottom, respectively.

$$R = \frac{1}{T_0}\int [U_b(T) - U_t(T)]\mathrm{d}T \quad (2)$$

The R values of the prepared composite fabric are shown in Fig. 6(a)–(c). Regardless of which coating material is used, the electrospraying time is directly correlated with the R value, indicating that the unidirectional water transport capacity of the composite fabric is enhanced with the increase in the spraying amount. This is because the difference in wettability and roughness on both sides of the fabric increases with the increase in spraying time. For the electrospraying time of 1 h, the cotton and hemp composite fabrics already show effective unidirectional transport capacity, whereas the R values of the modal composite fabrics are negative, indicating that water transport from the top to the bottom is not encouraged, and water diffusion occurs at the top. This can be attributed to the high hygroscopicity of the modal fabric, the small wettability gradient force, and the thrust generated by the hydrophobic layer is not sufficient to prevent the diffusion of water droplets on the upper surface. When the electrospraying time increases to 3 h, the R values of PVC-M and PVDF-M are 729.7% and 309.7%, respectively.

Fig. 6(d)–(i) shows the relative changes in the moisture content on the hydrophobic and hydrophilic sides of each composite fabric prepared using an electrostatic spraying time of 3 h. When water contacts the upper surface (the hydrophobic side), the moisture content on both sides increases and quickly reaches the maximum value. Finally, the moisture content of the lower surface becomes twice or more than that of the upper surface, indicating that water can be transferred from the upper surface to the lower surface because of a strong driving force. Moreover, the larger the gap between the moisture content curves on both sides of the fabric, the higher the unidirectional moisture conduction performance of the fabric. Notably, the gap between the moisture content curves of the modal composite fabric is smaller than that of other fabrics, so the unidirectional moisture conduction performance is relatively poor. This result is consistent with the R value comparison.

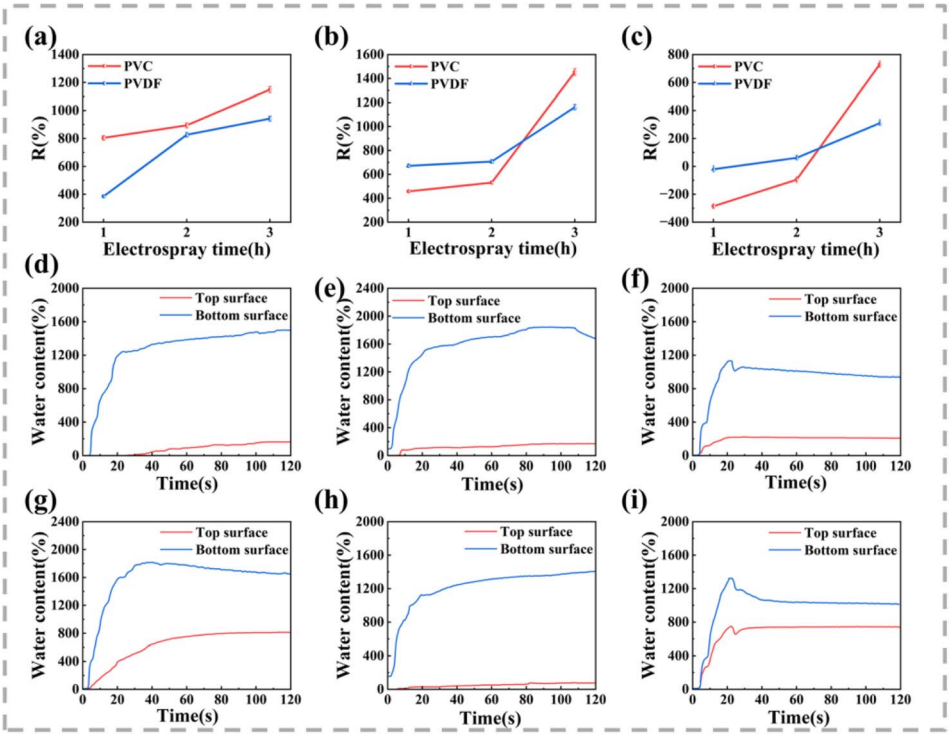

Fig. 6 Diffusion diameter and water content of the (a, d and g) cotton, (b, e and h) hemp, and (c, f and i) modal composite fabrics after electrospraying for 3 h: (a–c) *R* value, (d–f) MMT results after PVC treatment, and (g–i) MMT results after PVDF treatment.

3.5. Mechanism of directional water transport

To further elucidate the directional water conduction process in the composite fabric, PVC-H-3 was used as an example to visualize the water transport. When the hydrophobic side was facing upward (Fig. 7(a)), the water droplet immediately transferred from the hydrophobic side to the hydrophilic side. In contrast, when the water droplet fell on the hydrophilic side (Fig. 7(b)), the wetted area of the droplet gradually increased over time, and ultimately, the droplet only spread on the upper surface without penetrating the fabric. These results confirmed that the water droplet could only be transported from the electrosprayed surface to the untreated surface, demonstrating that the wettability gradient across the fabric thickness promotes unidirectional water conduction behavior.

Based on the above results, we proposed a mechanism to explain the unidirectional water conduction phenomenon. As shown in Fig. 7(c), when a water droplet falls on the hydrophobic upper surface, it is subjected to two opposing forces in the vertical direction:[25] hydrostatic pressure (F_{HP}) and a hydrophobic force (F_{HF}). F_{HP} is proportional to the height of the water droplet from the material, providing the water droplet with the force to penetrate the hydrophobic layer. The calculation is expressed as follows: $F_{HP} = \rho gh$, where h represents the height of the water droplet from the fabric surface, g represents the acceleration of gravity, and ρ is the density of water. Conversely, F_{HF} prevents water from penetrating. When the water droplet first contacts the upper surface, F_{HP} is weak and the water droplet cannot pass through the hydrophobic layer. As the height of the water droplet increases with the accumulation of water, F_{HP} increases accordingly. When $F_{HP} > F_{HF}$, the water passes through the hydrophobic layer and contacts the hydrophilic side. Then, because of the capillary force F_{CF}, the water drop quickly penetrates and transfers to the hydrophilic side and diffuses, thus achieving continuous transmission of water droplets from the hydrophobic side to the hydrophilic side. However, when the water droplet falls on the hydrophilic side, the capillary force immediately causes the water droplet to diffuse in the horizontal direction. At this time, F_{HP} also promotes water penetration, but when the water reaches the hydrophobic side, F_{HF} prevents further penetration.

3.6. Air permeability properties

Fig. 8(a)–(c) displays the air permeability of each fabric prepared with different electrospraying times. It can be seen that the air permeability decreases with the increase in the thickness of the hydrophobic layer, showing a change trend consistent with the MMT results. As the electrospraying time increases, the pores on the surface of the fabric are gradually covered, thereby hindering the passage of air and reducing air permeability. Nevertheless, compared with other studies, this type of fabric still shows higher permeability.[26] In addition to the high MMT performance, a high WVT rate is an important feature. Fig. 8(d)–(f) shows the WVT rate of each fabric in the forward (from electrosprayed side to untreated side) and reverse directions after electrospraying for 3 h. All fabrics have high water vapor permeability. Compared with the untreated fabric, the forward WVT rate is improved, and the forward rate is greater than the reverse rate. This may be because water vapor can

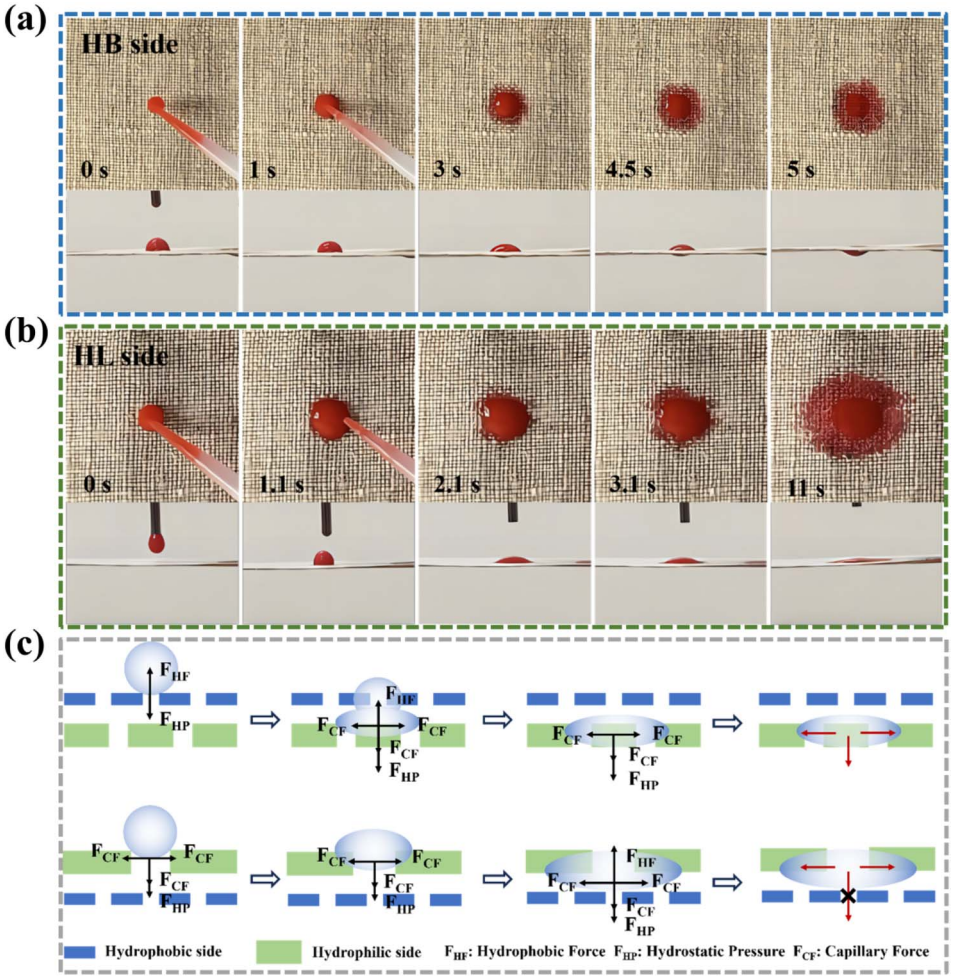

Fig. 7 Wetting behavior of ink droplets on (a) HL and (b) HB surfaces as viewed from the top and side, respectively (c) Schematic diagram of directional water transport mechanism (HL represents the hydrophilic side and HB represents the hydrophobic side).

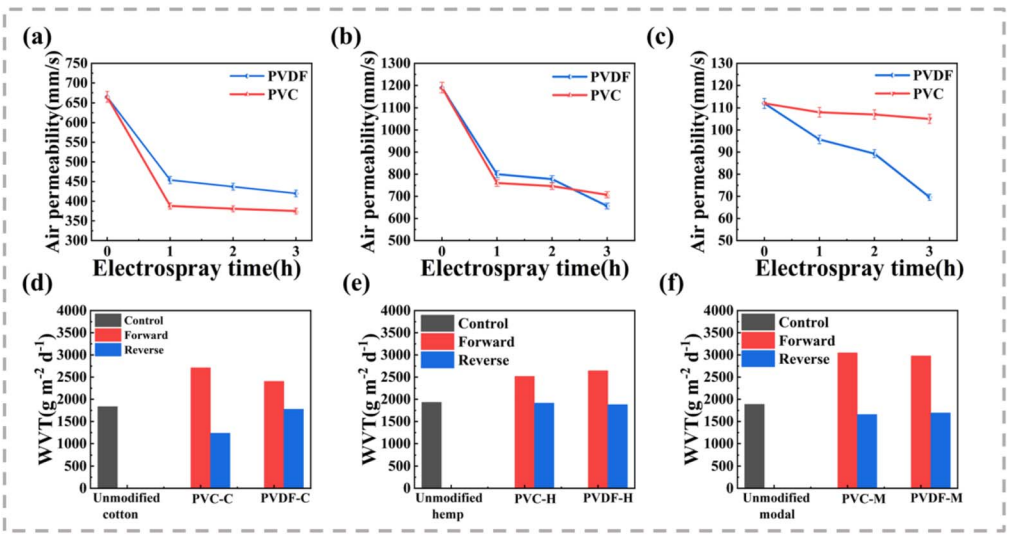

Fig. 8 (a–c) Air permeability of composite fabrics at different electrospraying times, (a) cotton, (b) hemp and (c) modal. (d–f) WVT rate of composite fabrics at 3 h of electrospraying, (d) cotton, (e) hemp and (f) modal.

easily pass through the sprayed side and become quickly absorbed by the unsprayed side, where it can evaporate into the test environment. Conversely, water vapor immediately becomes absorbed and diffuses and is not easily evaporated. The difference in wettability is also an important reason for the difference in WVT rate. Moreover, a normal adult sweats 1200–2000 g d^{-1} during regular exercise, which means that a fabric with a WVT rate of 2000 g m^{-2} d^{-1} can ensure comfortability.[27,28] The WVT rates of all fabrics in the positive direction are greater than this value, indicating that they have broad application prospects in comfortable moisture-wicking textiles.

4. Conclusions

In this study, fabrics with rapid unidirectional moisture-conducting functionality were prepared by electrospraying hydrophobic polymer coatings on hydrophilic fabric surfaces. Uniform and strongly adherent coatings were produced, providing wettability differences and roughness differences across the thickness direction of the fabrics and driving water to spontaneously permeate from the hydrophobic side to the hydrophilic side without reverse penetration. The unidirectional moisture-conducting ability of the obtained functional fabrics can be regulated by controlling the electrospraying time. This technique is simple, low-cost, and easily scalable, offering valuable insights for the production of more efficient, high-performance unidirectional moisture-wicking fabrics.

Data availability

The original data of the study are included in the article. Further inquiries can be directed to the corresponding authors.

Author contributions

Shumin Bi: methodology, investigation, formal analysis, writing – original draft. Yueru Yang: conceptualization, investigation, data curation. Guangling Pei: investigation, supervision, validation. Tianci Yang: sample data analysis. Shui Hu: validation, supervision, resources, funding acquisition. Qingxiu Jia: conceptualization, writing – review & editing, validation, resources.

Conflicts of interest

The authors declare no conflicts of interest.

Acknowledgements

The authors sincerely acknowledge the financial support from the Project of Top Young Talents of Beijing Excellent Talents Training Program (2018), the Beijing Nova Program (20220484213), and the Innovation Teambuilding Program of Beijing Institute of Fashion Technology (BIFTTD201904).

References

1 X. Li, W. Guo and P. Hsu, *Adv. Mater.*, 2023, **36**, e2209825.
2 S. F. Neves, J. B. L. M. Campos and T. S. Mayor, *Appl. Therm. Eng.*, 2017, **117**, 109–121.
3 C.-I. Su, J.-X. Fang, X.-H. Chen and W.-Y. Wu, *Text. Res. J.*, 2007, **77**, 764–769.
4 Y. Lin, X. Liu, A. A. Babar, X. Wang, J. Yu and B. Ding, *ACS Appl. Mater. Interfaces*, 2023, **15**, 53105–53112.
5 J. Chen, Y. Rao, X. Zhu, J. Wang, X. Tang, S. Feng, F. Zhang, Z. Zhong and W. Xing, *J. Membr. Sci.*, 2022, **662**, 121006.
6 Q. Zhang, Y. Li, Y. Yan, X. Zhang, D. Tian and L. Jiang, *ACS Nano*, 2020, **14**, 7287–7296.
7 Y. Song, X. Chen, K. Xu, H. Li, Y. Xu, H. Wu, J. Wu and C. Huang, *ACS Sustain. Chem. Eng.*, 2019, **7**, 19679–19685.
8 Q. Zhen, H. Zhang, H. Li, J.-Q. Cui, J. Cheng and Y. Liu, *ACS Appl. Polym. Mater.*, 2021, **3**, 3354–3362.
9 G. Huang, Y. Jin, L. Huo, S. Yuan, R. Zhao, J. Zhao, Z. Li and Y. Li, *ACS Appl. Mater. Interfaces*, 2021, **13**, 51708–51717.
10 Y. Pu, J. Yang, S. J. Russell and X. Ning, *Cellulose*, 2021, **28**, 4427–4438.
11 Y. Tan, K. Fang, W. Chen, Q. Shi and C. Zhang, *Ind. Crops Prod.*, 2024, **209**, 118034.
12 F. Sun, Z. Chen, L. Zhu, Z. Du, X. Wang and M. Naebe, *Coatings*, 2017, **7**, 132.
13 Y. Tian, Y. Zhang, Y. Yu, K. Zhao, X. Hou and Y. Zhang, *Colloids Surf., A*, 2023, **664**, 131131.
14 H. Yang, Y. Wang, Z. Fan, Q. Jia, S. Hu and G. Pei, *Polym. Eng. Sci.*, 2024, **64**, 3617–3628.
15 J. Xu, B. Xin, Z. Chen, Y. Liu, Y. Zheng and F. Zhang, *RSC Adv.*, 2019, **9**, 16754–16766.
16 Z. Zhang, Y. Meng, H. Niu and H. Zhou, *Surf. Coat. Technol.*, 2023, **468**, 129773.
17 K. Huang, Y. Si, H. Wu, Y. Chen, S. Zhang, S. Shi, C. Guo and J. Hu, *ACS Appl. Mater. Interfaces*, 2023, **16**, 1899–1910.
18 V. Vatanpour, B. Kose-Mutlu and I. Koyuncu, *Desalination*, 2022, **533**, 115765.
19 L. Chen, A. A. Babar, G. Huang, J. Zhao, W. Yan, H. Yu, Q. Feng and X. Wang, *J. Colloid Interface Sci.*, 2023, **645**, 200–209.
20 Y. Cheng, J. Wang, X. Lu and C. Wang, *Nano Energy*, 2023, **117**, 108852.
21 H. Wang, W. Wang, H. Wang, X. Jin, J. Li, H. Wang, H. Zhou, H. Niu and T. Lin, *Appl. Surf. Sci.*, 2018, **455**, 924–930.
22 H. Wang, W. Wang, H. Wang, X. Jin, J. Li and Z. Zhu, *Mater. Lett.*, 2018, **215**, 110–113.
23 Y. He, D. Wang, Q. Li, L. Huang and H. Bao, *J. Wuhan Univ. Technol., Mater. Sci. Ed.*, 2020, **35**, 677–681.
24 H. Wang, W. Wang, H. Wang, X. Jin, J. Li and Z. Zhu, *ACS Appl. Mater. Interfaces*, 2018, **10**, 32792–32800.
25 J. Wu, N. Wang, L. Wang, H. Dong, Y. Zhao and L. Jiang, *Soft Matter*, 2012, **8**, 5996–5999.
26 H. Zhao, Z. Fan, C. Jia and Z. Cai, *Cellulose*, 2023, **30**, 3351–3361.
27 Y. Zhang, T.-T. Li, H.-T. Ren, F. Sun, Q. Lin, J.-H. Lin and C.-W. Lou, *RSC Adv.*, 2020, **10**, 3529–3538.
28 J. Ju, Z. Shi, N. Deng, Y. Liang, W. Kang and B. Cheng, *RSC Adv.*, 2017, **7**, 32155–32163.